Journal of Pharmaceutical Analysis 13 (2023) 1153–1167

Contents lists available at ScienceDirect

Journal of Pharmaceutical Analysis

journal homepage: www.elsevier.com/locate/jpa

Original article

Protective effects of dioscin against Parkinson's disease via regulating bile acid metabolism through remodeling gut microbiome/GLP-1 signaling

Zhang Mao [a, 1], Haochen Hui [a, 1], Xuerong Zhao [a], Lina Xu [a], Yan Qi [a], Lianhong Yin [a], Liping Qu [b, ***], Lan Han [c, **], Jinyong Peng [a, d, *]

[a] Department of Pharmaceutical Analysis, College of Pharmacy, Dalian Medical University, Dalian, Shenyang, 116044, China
[b] Innovation Materials Research and Development Center, Botanee Research Institute, Yunnan Botanee Bio-technology Group Co., Ltd., Kunming, 650106, China
[c] Department of Traditional Chinese Medicine Pharmacology, School of Pharmacy, Anhui University of Chinese Medicine, Hefei, 230012, China
[d] Department of Pharmacology, School of Pharmacy, Weifang Medical University, Weifang, Shandong, 261053, China

ARTICLE INFO

Article history:
Received 15 February 2023
Received in revised form
30 May 2023
Accepted 13 June 2023
Available online 16 June 2023

Keywords:
Parkinson's disease
Dioscin
Gut microbiota
Bile acid metabolism
GLP-1

ABSTRACT

It is necessary to explore potent therapeutic agents via regulating gut microbiota and metabolism to combat Parkinson's disease (PD). Dioscin, a bioactive steroidal saponin, shows various activities. However, its effects and mechanisms against PD are limited. In this study, dioscin dramatically alleviated neuroinflammation and oxidative stress, and restored the disorders of mice induced by 1-methyl-4-phenyl-1,2,3,6-tetrahydropyridine (MPTP). 16 S rDNA sequencing assay demonstrated that dioscin reversed MPTP-induced gut dysbiosis to decrease *Firmicutes*-to-*Bacteroidetes* ratio and the abundances of *Enterococcus*, *Streptococcus*, *Bacteroides* and *Lactobacillus genera*, which further inhibited bile salt hydrolase (BSH) activity and blocked bile acid (BA) deconjugation. Fecal microbiome transplantation test showed that the *anti*-PD effect of dioscin was gut microbiota-dependent. In addition, non-targeted fecal metabolomics assays revealed many differential metabolites in adjusting steroid biosynthesis and primary bile acid biosynthesis. Moreover, targeted bile acid metabolomics assay indicated that dioscin increased the levels of ursodeoxycholic acid, tauroursodeoxycholic acid, taurodeoxycholic acid and β-muricholic acid in feces and serum. In addition, ursodeoxycholic acid administration markedly improved the protective effects of dioscin against PD in mice. Mechanistic test indicated that dioscin significantly up-regulated the levels of takeda G protein-coupled receptor 5 (TGR5), glucagon-like peptide-1 receptor (GLP-1R), GLP-1, superoxide dismutase (SOD), and down-regulated NADPH oxidases 2 (NOX2) and nuclear factor-kappaB (NF-κB) levels. Our data indicated that dioscin ameliorated PD phenotype by restoring gut dysbiosis and regulating bile acid-mediated oxidative stress and neuroinflammation via targeting GLP-1 signal in MPTP-induced PD mice, suggesting that the compound should be considered as a prebiotic agent to treat PD in the future.

1. Introduction

Parkinson's disease (PD), one of the most prevalent neurodegenerative diseases, is characterized by dopaminergic neurons in substantia nigra pars compacta [1]. The incidence of PD has steadily risen in recent years and become a major source of health deterioration in the elderly [2,3].

The main pathological changes of PD are the degeneration and death of dopaminergic neurons, leading to the decreased dopamine (DA) levels in the substantia nigra striatum pathway [4]. The causes

Peer review under responsibility of Xi'an Jiaotong University.
* Corresponding author. Department of Pharmaceutical Analysis, College of Pharmacy, Dalian Medical University, Dalian, Shenyang, 116044, China.
** Corresponding author.
*** Corresponding author.
E-mail addresses: quliping@winona.cn (L. Qu), hanlan56@ahtcm.edu.cn (L. Han), jinyongpeng2008@126.com (J. Peng).
[1] Both authors equally contributed to this work.

https://doi.org/10.1016/j.jpha.2023.06.007

on substantia nigra striatum lesions are not entirely known [5,6]. Oxidative stress plays important roles in the degeneration of dopamine neurons and PD development. There are both enzymatic and nonenzymatic antioxidant defense systems to protect brain from oxidative damage [7]. PD is closely related to oxidative damage mediated by free radicals [8]. Reactive oxygen species (ROS) can affect DNA, which is more likely to occur under oxidative stress in substantia nigra [9,10]. Similarly, inflammation also plays an essential role during the pathological process of PD [2]. Inflammatory factors and immune cells can increase blood brain barrier (BBB) permeability and suppress enzymatic function, leading to neurodegeneration [11]. Hence, the ability on controlling oxidative stress and inflammation has profound meaning in identifying new antioxidant and anti-inflammatory medicines for PD therapy.

To maintain metabolic homeostasis, gut microbiota can influence the composition, diversity and function of microbiota. Hence, microbial composition and host metabolic disorders can cause various diseases. Recently, powerful evidences have found that the abundances of *Verrucomicrobiaceae*, *Lactobacillaceae* and *Lactobacillus* in PD patients are high [11,12]. Meanwhile, the abundances of other species such as *Enterococcus* and *Lactobacillus* can trigger levodopa degradation pathways in gut and ultimately lead to high drug dosages in clinical practice [13], suggesting that microflora dysfunction plays an essential role in PD-related neurodegeneration, and alteration of gut microbiota might be recognized as targets. Some studies have focused on gut microbiota and the progression of neurodegenerative diseases [14]. However, exploration of effective compound to prevent PD via adjusting microbiome and metabolism is necessary.

Metabolomics, a rapidly evolving tool, is targeted to define small molecular metabolites in biological samples. As the dominant downstream products of cholesterol catabolism, biosynthesis or excretion of bile acids (BAs) is crucial for the maintenance of cholesterol homeostasis [15,16]. Recently, robust evidence has demonstrated that bile acid signaling has an essential role in the central nervous system, and some BAs can exert neuroprotective potential in neurological diseases [17–19]. Intraperitoneal injection of ursodeoxycholic acid (UDCA) can protect rotenone-induced PD rats [20]. Tauroursodeoxycholic acid (TUDCA) can downregulate Parkin level in mice induced by 1-methyl-4-phenyl-1,2,3,6-tetrahydropyridine (MPTP) [21]. Thus, controlling gut metabolites should be a useful method to treat PD.

Recently, the interaction between brain and gut microbiota has been confirmed. Glucagon-like peptide-1 (GLP-1), a key mediator in regulating gut microbiota [22], plays a beneficial role in brain by binding to its receptor (GLP-1R) [23]. A study has revealed that lixisenatide and liraglutide, which are GLP-1 analogs, have protective effects on improving motor function in MPTP rodent model of PD [24]. Moreover, GLP-1 can influence neuroinflammation and enhance neural structure in microglia experiments [25]. A large number of G protein-coupled receptors (GPCRs) are distributed on the surface of intestinal endocrine cells. As a member of GPCR subfamily, TGR5 is highly involved in energy homeostasis, bile acid balance and glucose metabolism. It has been reported that stirring TGR5 can promote GLP-1 secretion and regulate glycolipid metabolism [26]. In addition, up-regulated GLP-1 can increase the levels of inducible nitric oxide synthase (iNOS) and NADPH oxidases 2 (NOX2) in diabetic rats under cerebral ischemia/reperfusion injury condition [27]. Enhancing GLP-1 level can markedly hinder nuclear factor-kappaB (NF-κB) pathway and alleviate Cigarette smoking-induced neuroinflammation [28]. Therefore, GLP-1 might be involved in the pathogenesis of PD via regulating microbiota-gut-brain axis, neuroinflammation and oxidative stress.

Dioscin, a natural steroidal saponin, exerts excellent anti-inflammatory and anti-oxidant activities [29–31]. Our studies have shown that dioscin can attenuate cerebral ischemia/reperfusion injury [32], and protect brain aging by decreasing oxidative stress [33]. It has been reported that dioscin-zein-carboxymethyl cellulose (CMC) complexes can prevent PD in *Caenorhabditis elegans* [34]. Interestingly, oral administration of dioscin is retained in intestine for an extended time, and most of it is excreted from intestine in a prototype mode [35]. Recent report has confirmed that dioscin can inhibit cisplatin-induced gut microbiota dysbiosis, relieve the connection between ileal epithelial cells, and increase mucus secretion to alleviate cisplatin-induced mucositis [36]. In addition, dioscin can regulate the abundance of *Muribaculaceae* to improve inflammation in enteric nervous system microenvironment in slow transit constipation mice [37]. Thus, the purpose of the study was to evaluate the pharmacological effect of dioscin against PD, and then the methods of 16 S ribosomal DNA-based microbiota analysis and metabolomics profiling were used to focus on the therapeutic mechanism.

2. Materials and methods

2.1. Chemicals

Pure dioscin was produced in our laboratory and dissolved in 0.5% CMC-Na for intragastric administration. Glutathione (GSH) and superoxide dismutase (SOD) kits were purchased from Nanjing Jiancheng Biotechnology Company (Nanjing, China). Tissue protein extraction kit was purchased from Key GEN Biotech. Co., Ltd. (Nanjing, China). MPTP reagent was purchased from Aladdin Biological Reagent Company (Shanghai, China). UDCA standard was obtained from Sigma Aldrich (Shanghai, China) and Steraloids (Shanghai, China). Triple antibiotics (vancomycin, ampicillin and metronidazole) were purchased from MedChemExpress (Shanghai, China).

2.2. Animals

Sixty male C57BL/6 J mice weighing 18–22 g (4–6 weeks old) were purchased from the Experimental Animal Center of Dalian Medical University (SCXK: 2013–0006). All animal care and laboratory procedures were carried out in accordance with the relevant regulations of the "Use and Care of Laboratory Animals" and approved by the Animal Care and Use Committee of Dalian Medical University (Ethical number: AEE21010). Animals were kept in a controlled environment with a 12 h light schedule, with temperature of 20 ± 3 °C and relative humidity of 60% ± 10%.

2.3. Pharmacological treatment and design

After adapting to the environment for 1 week, the mice were randomly divided into control group, MPTP group, MPTP + dioscin groups and MPTP + 3,4-dihydroxyphenylalanine (L-DOPA) group with 12 mice in each group. The mice in MPTP group were intraperitoneally injected with MPTP (30 mg/kg/day) for 7 consecutive days, and same volume of normal saline was injected intraperitoneally on the 8th to 28th days. The animals in MPTP + dioscin and L-DOPA groups were administered intragastrically with dioscin (20, 40, and 80 mg/kg), and L-DOPA (8.4 mg/kg) on the 8th to 28th days [35,36]. The control mice were administered with the equal volume of saline every day for 28 consecutive days. The experimental procedures are shown in Fig. 1A. For *anti*-PD effect of UDCA combined with dioscin experiment, C57 mice were divided into control group, MPTP group, MPTP + UDCA (50 mg/kg) group, MPTP + dioscin (80 mg/kg) group and MPTP + UDCA group. MPTP modeling and dioscin administration methods were conducted as above. UDCA was administered intraperitoneally for 2 weeks.

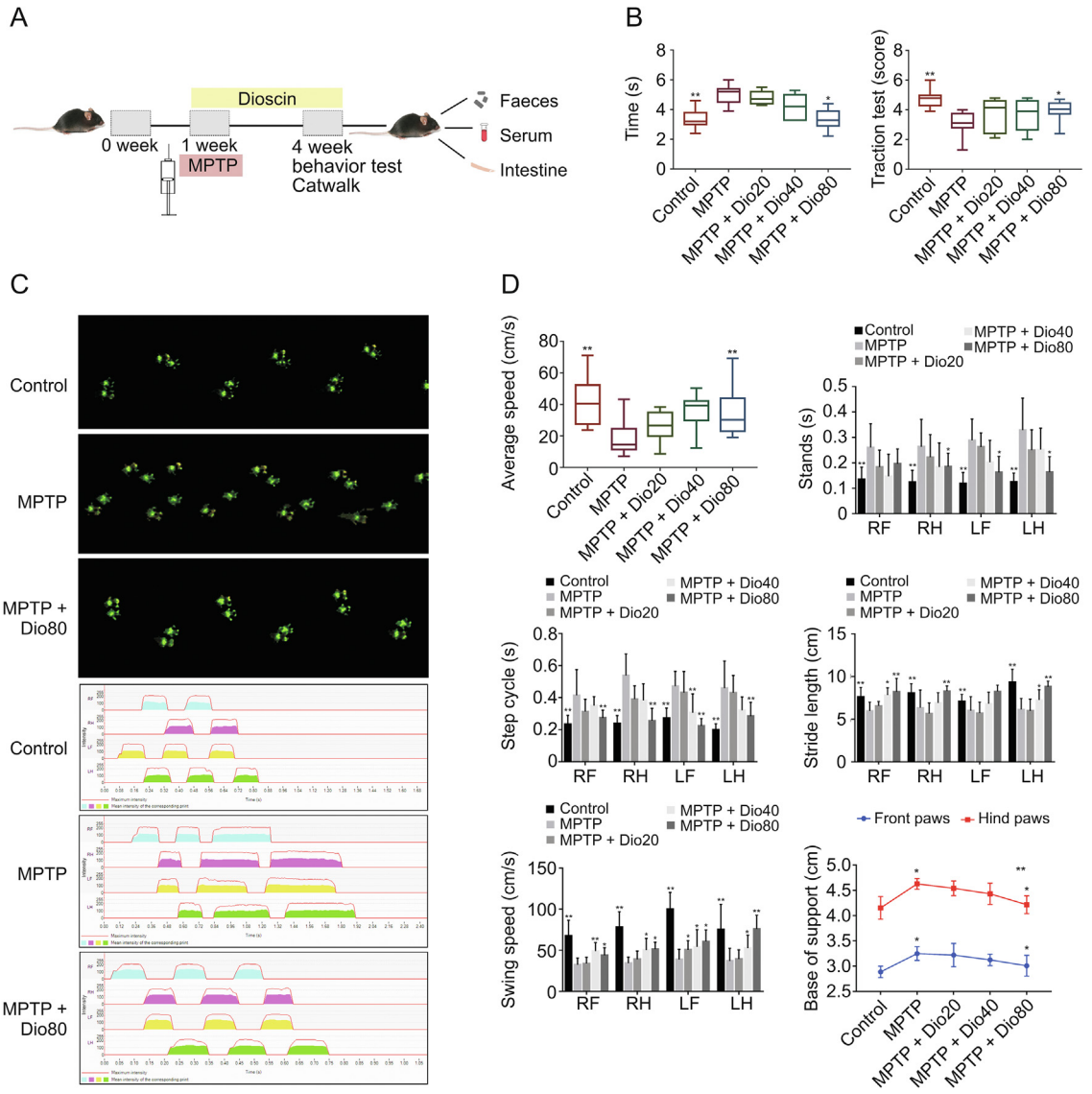

Fig. 1. Dioscin improves the behavior of mice induced by 1-methyl-4-phenyl-1,2,3,6-tetrahydropyridine (MPTP). (A) The group assignments and time line of the experimental process. (B) Motor behavior of mice after dioscin treatment on MPTP-induced Parkinson's disease (PD) model, including pole test and traction test. (C) CatWalk print and mean intensity of the corresponding print of mice after dioscin treatment on MPTP-induced PD model. The upper panel (green prints in black background) shows the digitized prints, and the lower panel shows walking pattern and individual paws (RF: right front; RH: right hind; LF: left front; and LH: left hind). (D) The mice gait behavior indicators change after dioscin treatment on MPTP-induced PD model, including average speed, stands, step cycle, stride length, swing speeds and the base of support. All data are given as mean ± standard deviation (SD) ($n = 8$). $^{*}P < 0.05$ and $^{**}P < 0.01$ compared with MPTP group.

2.4. Pole and traction tests

The mice were placed on the top of a homemade climbing pole foam ball, and the times spent climbing down the metal rod from the small ball (turning time), the upper part, the lower part and the whole rod were recorded. In traction test, all mice were hung on a suspension wire, and the specific evaluation criteria were as follows. Two hind limbs of mice hooked on the electric wire were scored as 3 points. The mice with only one hind limb hooked on the wire were counted as 2 points, and the mice without a hind limb hooked on the wire were counted as 1 point. The incubation period of the three groups of mice from hanging to falling was recorded.

2.5. Gait analysis

Catwalk XT (Noldus, Wageningen, Netherlands) was used to assess the natural motor behavior and coordination of mice. The training was conducted for 3 days before the experiment. During detection, the mice were allowed to pass through the detection channel of the set length freely. The footprints were processed efficiently using footprint refraction technology with an internal light source, and each mouse was tested three times.

2.6. Histopathological and immunochemical examination

Brain tissues were harvested, washed and fixed in 4% paraformaldehyde at 4 °C for 12 h. Next, the sample was embedded in paraffin, sliced (5 μm) and stained with hematoxylin and eosin (H&E). Immunohistochemical assay kit was used to detect tyrosine hydroxylase (TH) expression.

2.7. Immunofluorescence examination

Paraffin sections of mice were dewaxed and processed for staining as Section 2.6. Then, the sections of substantia nigra and striatum tissues were incubated with ionized calcium bindingadaptor

molecule-1 (IBA-1) and glial fibrillary acidic protein (GFAP) antibodies at 4 °C in a humidified chamber overnight. Then, the labeled secondary antibody (1:500, *V*/*V*) was used to incubate the tissue section at room temperature for 1 h. After incubation with 4',6-diamidino-2-phenylindole (DAPI) (1:100, *V*/*V*) at room temperature for 30 min, 5 visual fields were observed by TE2000U fluorescence microscope (Nikon, Tokyo, Japan), and the positive cells were counted.

2.8. Antioxidant assay

Malondialdehyde (MDA), glutathione (GSH)/glutathione synthase (GSS) and superoxide dismutase (SOD) levels in tissues were detected using the kits. The level of intracellular reactive oxygen species (ROS) was detected by dihydroethidium (DHE) staining, in which the cryosection was incubated with dihydroergotamine (DHE) (10 μM) at 37 °C. The results were obtained by a SpectraMax Microplate Reader (Molecular Devices, San Jose, CA, USA).

2.9. Fecal bile salt hydrolase (BSH) activity

BSH activity was tested as previously described [38], and taurine was considered as a standard and the detection absorbance was 570 nm.

2.10. Fecal microbiota transplantation (FMT) test

In FMT test, the recipient mice was conducted as previously reported [39]. The specific operation method was in Supplementary data.

2.11. Metabolomics profiling of fecal samples

Fecal samples totaling 100 ± 1 mg were analyzed. For gas chromatography-mass spectrometry (GC-MS) and liquid chromatography-mass spectrometry (LC-MS) assays, the samples were extracted as previously described [40]. An Agilent 7890 gas chromatograph coupled with a time-of-flight mass spectrometer was applied, and the specific analysis conditions were conducted as described in a previous study [41]. A 1,290 Infinity series ultra-performance liquid chromatography (UPLC) system (Agilent Technologies, Santa Clara, CA, USA) equipped with a UPLC BEH Amide column (2.1 mm × 100 mm, 1.7 μm) was used, and the analysis conditions were applied according to previous studies [42–44]. The MS analysis conditions are shown in the Supplementary data.

2.12. Targeted bile acid quantification

Bile acids were quantified by an Agilent 1290 infinity series UPLC system equipped with a Waters ACQUITY UPLC BEH C_{18} column ((Miford, MA, USA; 150 mm × 2.1 mm, 1.7 μm). The chromatographic conditions are shown in the Supplementary data. Metabolite extraction and method validation were performed according to a previous description [45].

2.13. Western blotting assay

Proteins from brain and ileum tissues were extracted and quantified. More experimental operation details are shown in the Supplementary data. The primary antibodies are listed in Table S1.

2.14. qPCR assay

Total RNA samples were extracted from brain and ileum tissues using TRIzol reagent. The sequences of the primers are shown in Table S2 and more details are shown in the Supplementary data.

2.15. Statistical analyses

The data are presented as the mean ± standard deviation (SD). GraphPad Prism 7.0 was used to analyze result. One-way ANOVA was adopted to compare the mean samples among multiple groups. $P < 0.05$ and $P < 0.01$ were considered statistically significant.

3. Results

3.1. Dioscin improved motor behavior in mice

The pole test in Figs. 1B and S1A showed that MPTP significantly induced bradykinesia in mice, whereas dioscin decreased the prolongation of descent time compared with MPTP group. In addition, the traction test results revealed that the mice in MPTP group received lower scores, which were increased by dioscin. As shown in Figs. 1C, 1D and S1B, the mice in control group traversed the walkway with short consistent steps, while the animals in MPTP group walked at a slower irregular pace with fewer steps per s. After dioscin treatment, the long uneven steps were decreased to consistent repetitive short steps. The stand phase revealed that the period of contact between all paws and the glass plate was decreased by dioscin compared with MPTP group. In addition, the stride length, average speed and swing speed were improved by the compound. Our results revealed that dioscin improved neuron viability and motor behavior in mice.

3.2. Dioscin improved neuron viability and oxidative stress

H&E staining in Fig. 2A showed that the corpus striatum with nuclear pyknosis and anachromasis was damaged, which was reduced by dioscin. As shown in Figs. 2B and C, TH levels were decreased in the substantia nigra and stratum of model mice, which were increased by dioscin. In addition, the activation of astrocytes and microglia based on IBA-1 and GFAP staining was increased in MPTP group compared with control group, which was reversed by the compound (Fig. 2D). As shown in Figs. 2E and F, the levels of SOD and MDA in serum, GSH/glutathione disulfide (GSSG) level, and ROS levels were all dramatically reversed by dioscin compared with MPTP group.

3.3. Dioscin remodeled gut microbiota composition in MPTP mice

16 S rDNA sequencing assay was applied to study gut microbiota (Supplementary data). The results of Chao1 index and operational taxonomic unit (OTU) numbers revealed that compared with MPTP group, the control and MPTP + Dio groups had higher microbial diversity (Figs. 3A, 3B, S2A, and S2B), and the results in Fig. 3C showed that there were 195 common OTUs between the three groups. Principal coordinate analysis (PcoA) showed that MPTP group had a different pattern of microbiota composition compared with control group, and a difference between MPTP and MPTP + Dio groups was found (Fig. 3D). The results of linear discriminant analysis (LDA) effect size (LEfSe) and Kyoto Encyclopedia of Genes and Genomes (KEGG) pathway analysis also showed that the microbial structure of gut microbiota in MPTP mice was reshaped by dioscin (Figs. S2C–F). The degree of bacterial taxonomic similarity on phylum level in Figs. 3E and F revealed three dominant phyla: *Firmicutes*, *Proteobacteria* and *Bacteroidetes*. Compared to control mice, MPTP-mice displayed a significant decrease in the relative abundance of *Firmicutes* and *Proteobacteria*, and a lower *Firmicutes*-to-*Proteobacteria* ratio, which were protected by dioscin. As shown in Figs. 3G–I, on class and order levels, the abundances of *Bacteroidia*, *Bifidobacteriales* and *Lactobacillales* were increased. Simultaneously, the decreased abundances of *Clostridia*, *Deltaproteobacteria*,

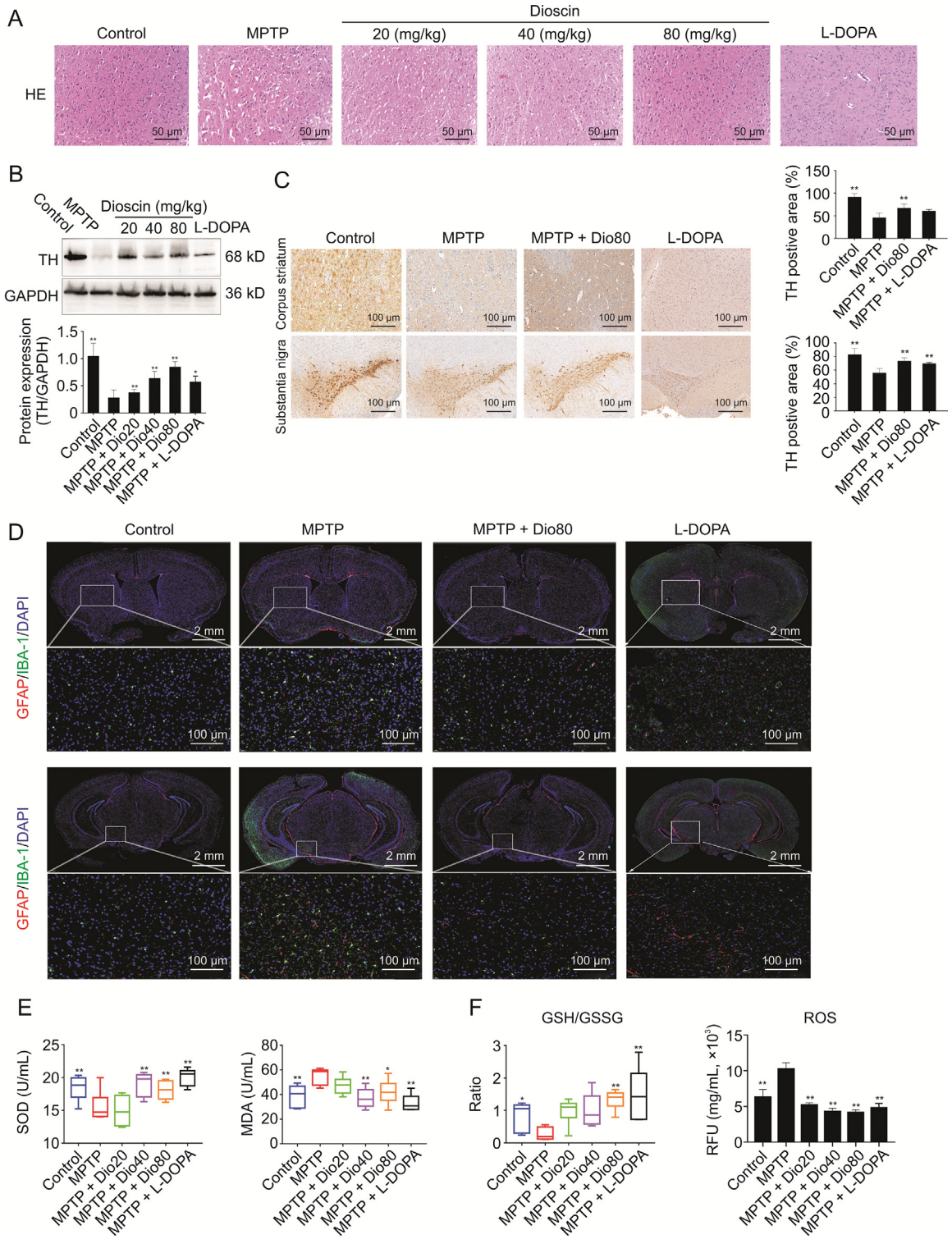

Fig. 2. Dioscin inhibits neuron viability and oxidative stress. (A) The histological changes of brain tissues after dioscin treatment on 1-methyl-4-phenyl-1,2,3,6-tetrahydropyridine (MPTP)-induced Parkinson's disease (PD) mice. (B) Western blotting of tyrosine hydroxylase (TH) in mice brain tissues after dioscin treatment on MPTP-induced PD mice ($n = 3$). (C) Immunohistochemistry assay of TH in mice brain tissues after dioscin treatment on MPTP-induced PD mice ($n = 3$). (D) Fluorescence semi-quantitative analysis of glial fibrillary acidic protein (GFAP) and ionized calcium bindingadaptor molecule-1 (IBA-1) expression in brain tissues after dioscin treatment on MPTP-induced PD mice ($n = 3$). (E) The levels of superoxide dismutase (SOD) and malondialdehyde (MDA) in brain tissues after dioscin treatment on MPTP-induced PD mice ($n = 6$). (F) The levels of glutathione (GSH)/glutathione disulfide (GSSG) and reactive oxygen species (ROS) in brain tissues after dioscin treatment on MPTP-induced PD mice ($n = 6$). Data are expressed as mean ± standard deviation (SD). $^{*}P < 0.05$ and $^{**}P < 0.01$ compared with MPTP group.

Gammaproteobacteria, *Clostridiales* and *Enterobacteriales* in MPTP group were reversed by dioscin. In addition, the increased abundances of *Enterococcus*, *Streptococcus*, *Bacteroides* and *Lactobacillus* were reversed by dioscin compared with model group on genus level. The results in Fig. 3J revealed that BSH activity was decreased by dioscin.

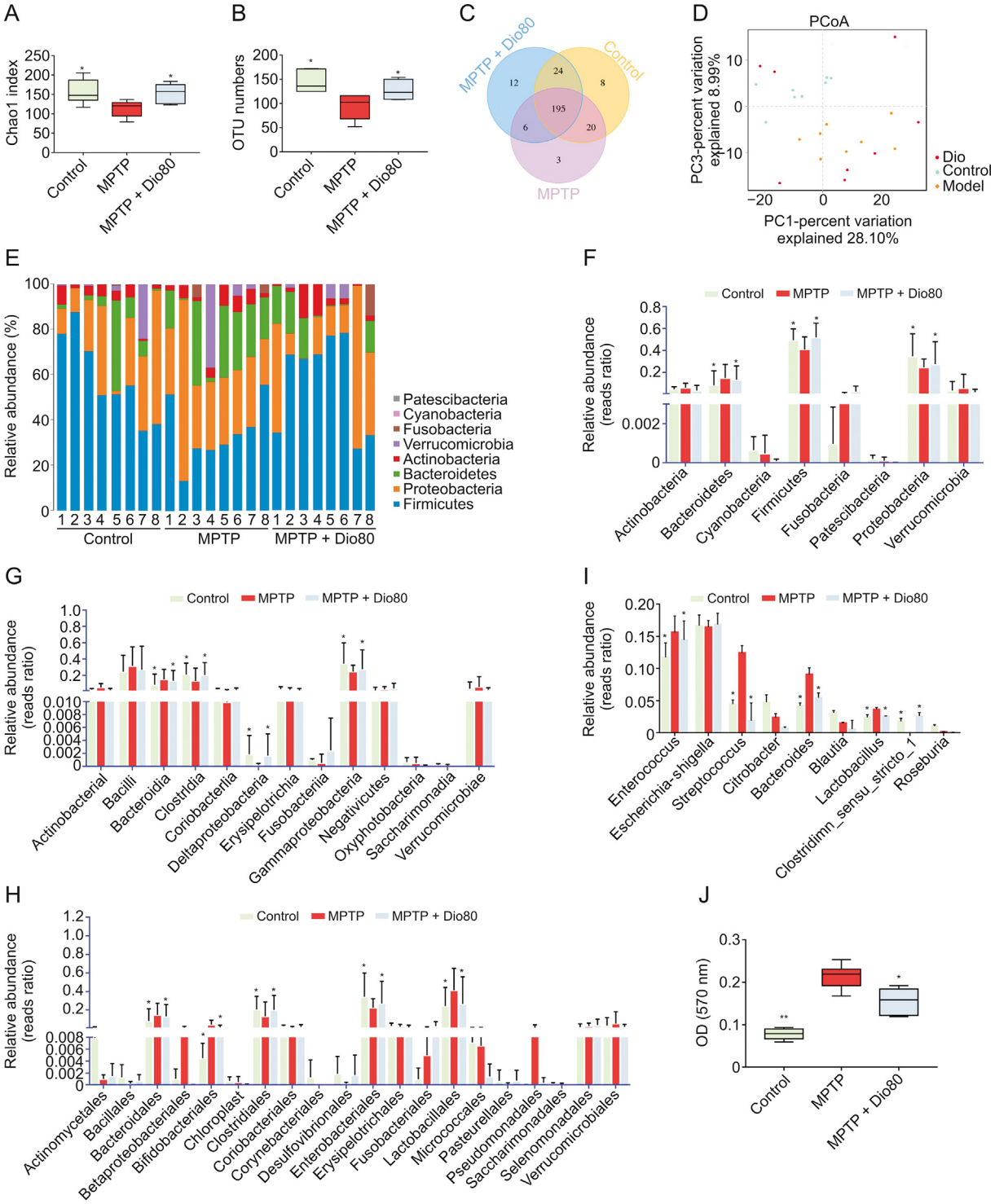

Fig. 3. Dioscin adjusts gut microbiota composition in 1-methyl-4-phenyl-1,2,3,6-tetrahydropyridine (MPTP) mice. (A) Chao1 index of control, MPTP and MPTP + Dio80 groups. (B) The operational taxonomic unit (OTU) numbers of control, MPTP and MPTP + Dio80 groups. In general, if the similarity between sequences exceeds 97% (species level), it can be defined as an OTU, with each OTU representing a species. (C) Venn diagram illustrates the common and differential microbiota among control, MPTP and MTPT + Dio80 groups. (D) UniFrac distance-based principal coordinate analysis (PCA). (E) Distribution of relative abundance of gut microbiota at the phylum level observed in the control, MPTP and MPTP + Dio80 groups. (F) Relative abundance of microbiota at phylum in control, MPTP and MPTP + Dio80 groups. (G) Relative abundance of microbiota at class in control, MPTP and MPTP + Dio80 groups. (H) Relative abundance of microbiota at order in control, MPTP and MPTP + Dio80 groups. (I) Relative abundance of microbiota at genus level in control, MPTP and MPTP + Dio80 groups. (J) Fecal bile salt hydrolase (BSH) activity. Data are expressed as mean ± standard deviation (SD) ($n = 6$). $^{*}P < 0.05$ and $^{**}P < 0.01$ compared with MPTP group.

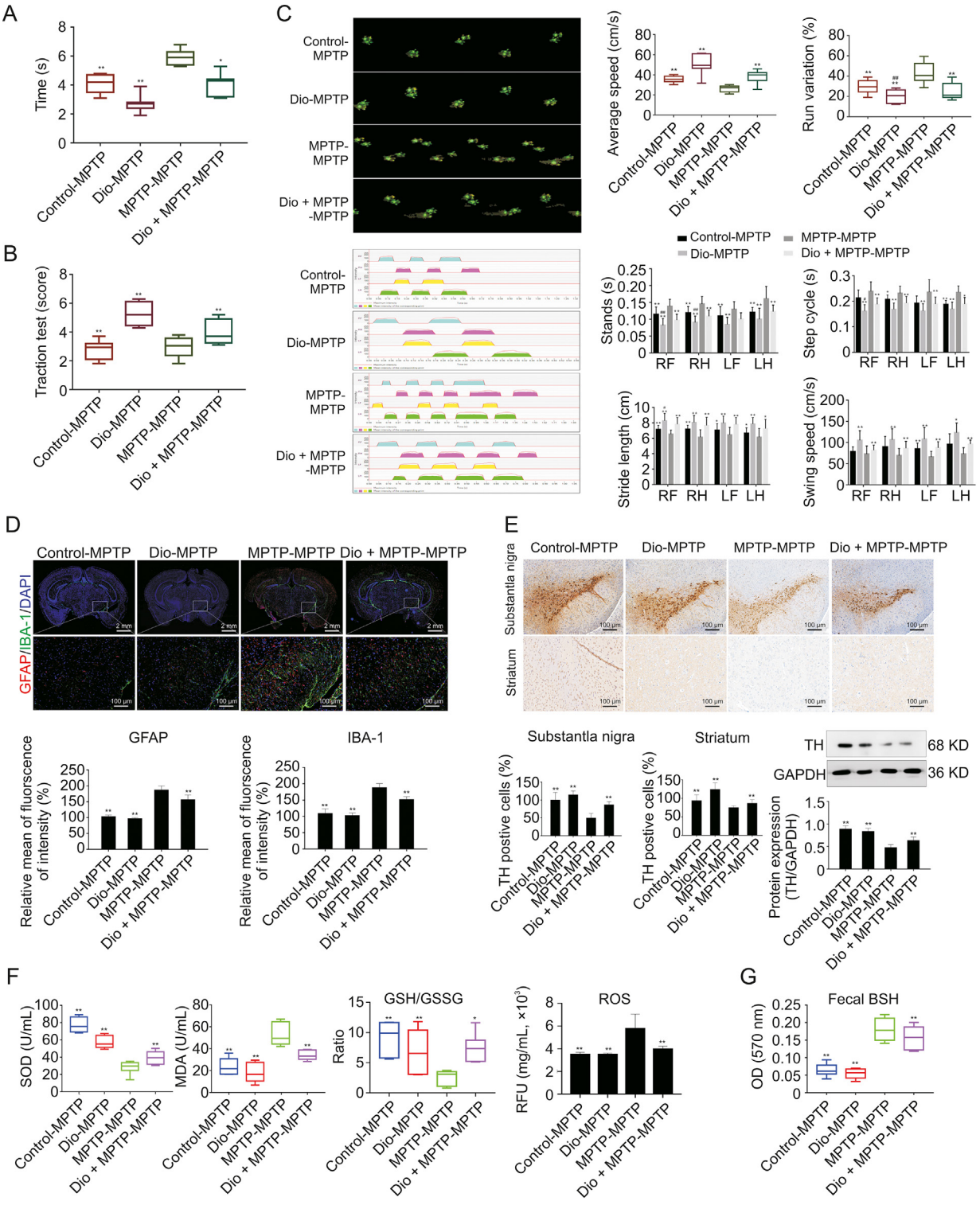

Fig. 4. Regulating effect of fecal transplantation from dioscin-treated mice to 1-methyl-4-phenyl-1,2,3,6-tetrahydropyridine (MPTP) mice. (A) Pole test of mice after fecal microbiota transplantation (FMT) treatment ($n = 8$). (B) Traction test of mice after FMT treatment ($n = 8$). (C) CatWalk print and mean intensity of the corresponding print of mice after FMT treatment ($n = 8$). The upper panel (green prints in black background) shows the digitized prints, and the lower panel shows walking pattern and individual paws (RF: right front, RH: right hind, LF: left front, and LH: left hind). And several parameters of CatWalk, i.e., the average speed, stride length, swing speed, run variation, stands, and step cycle, were affected variously in four groups. (D) Fluorescence semi-quantitative analysis of glial fibrillary acidic protein (GFAP) and ionized calcium bindingadaptor molecule-1 (IBA-1) expression in mice brain tissue after FMT treatment ($n = 3$). (E) Immunohistochemistry assay and western blotting assay of TH in mice brain tissues after FMT treatment ($n = 3$). (F) The levels of superoxide dismutase (SOD), malondialdehyde (MDA), glutathione (GSH)/glutathione synthase (GSS), reactive oxygen species (ROS) after FMT treatment ($n = 6$). (G) The levels of fecal bile salt hydrolase (BSH) activity after FMT treatment ($n = 6$). All data are given as mean ± standard deviation (SD). $^{*}P < 0.05$ and $^{**}P < 0.01$ compared with MPTP-MPTP group.

3.4. Dioscin fecal transplants exhibited a protective effect in MPTP mice

As shown in Figs. 4A and B, the mice in Dio-MPTP and Dio + MPTP-MPTP groups showed the decreased descent time and the increased traction score compared with MPTP-MPTP group. In Fig. 4C, the average speed, stride length and swing speed of mice were upregulated by Dio-MPTP treatment. Run variation, stands, and step cycle in Dio-MPTP group were decreased compared with MPTP-MPTP group. Interestingly, the mice in control-MPTP group displayed a significant impairment of gait disorders compared with MPTP-MPTP group. As shown in Fig. 4D, the expression levels of GFAP and IBA-1 were obviously increased in MPTP-MPTP group and decreased in control-MPTP, Dio-MPTP and Dio + MPTP-MPTP groups. Our results further demonstrated that fecal transfer of the mice in control, Dio and Dio + MPTP groups upregulated TH levels compared with MPTP-fed mice (Fig. 4E).In addtion, the results in Fig. 4F revealed that SOD, MDA, GSH/GSSG and ROS levels have statistically significant changes in Control-MPTP, Dio-MPTP, and Dio + MPTP-MPTP groups compared with MPTP-MPTP group. The results in Fig. 4G showed that BSH activities were decreased in Dio + MPTP-MPTP, Dio-MPTP and Control-MPTP groups compared with MPTP-MPTP group.

3.5. Dioscin recovered the fecal metabolome by untargeted metabolomic analysis

The results in Fig. 5A revealed that distinct separation of metabolites was observed among control, MPTP and MPTP + Dio

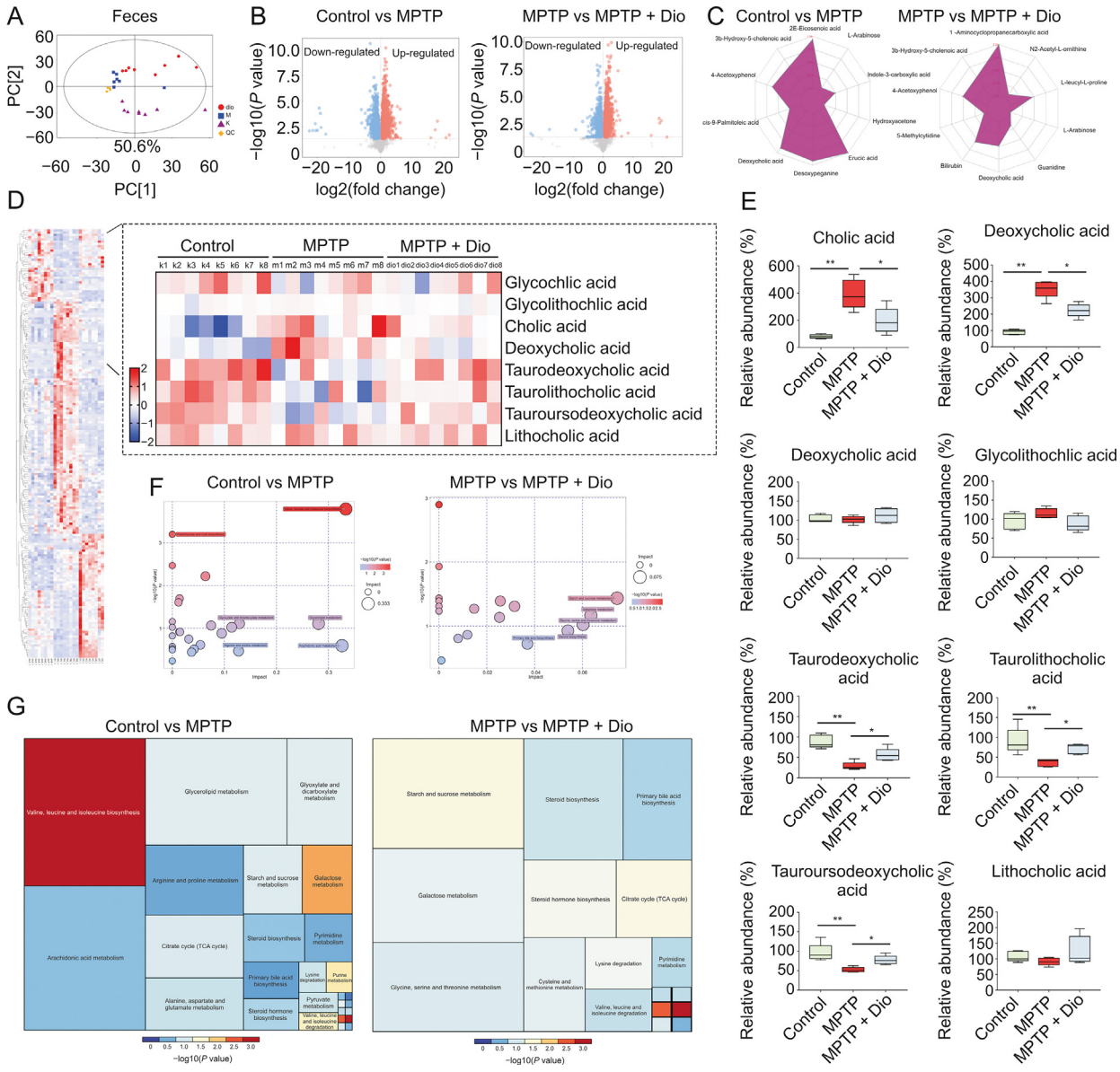

Fig. 5. Dioscin adjusts fecal metabolome by untargeted metabolomic analysis. (A) Principal components analysis (PCA) score plots for discriminating the fecal metabolome from control, 1-methyl-4-phenyl-1,2,3,6-tetrahydropyridine (MPTP), and MPTP + Dio groups. (B) Volcanic plot of differential metabolites among control, MPTP and MPTP + Dio groups. (C) Radar chart of differential metabolites among control, MPTP and MPTP + Dio groups. (D) Hierarchical clustering heat map of differential metabolites among control, MPTP and MPTP + Dio groups. (E) Some typical differential metabolites including cholic acid, deoxycholic acid, glycocholic acid, glycolithochilc acid, taurodeoxycholic acid, taurolithocholic acid, tauroursodeoxycholic acid and lithocholic acid among control, MPTP and MPTP + Dio groups. (F) Bubble plot of metabolites and significant pathway after dioscin treatment. (G) Tree map blot of metabolites and significant pathway after dioscin treatment. All data are given as mean ± standard deviation (SD) ($n = 6$). $^{*}P < 0.05$ and $^{**}P < 0.01$ compared with MPTP group.

groups. orthogonal projections to latent structures discriminant analysis (OPLS-DA) also showed distinct separation among the groups (Fig. S3A). The results in Fig. 5B indicated that many differential metabolites were detected in feces (Tables S3–S6). Notably, dioscin partially regulated the changes of L-arabinose, 4-acetoxyphenol, 3b-hydroxy-5-cholenoic acid and deoxycholic acid (Fig. 5C). In addition, the levels of cholic acid and deoxycholic acid were obviously elevated, and the levels of taurodeoxycholic acid, taurolithocholic acid and tauroursodeoxycholic acid were significantly decreased in MPTP group compared to control mice, which were reversed by dioscin (Figs. 5D and E). The bubble plot and treemap plot described the effects of dioscin on the responsive metabolites, and demonstrated the most significant pathway influenced by steroid biosynthesis and primary bile acid biosynthesis (Figs. 5F, 5G, and S3B). Specifically, crosstalk between gut microbiota and bile acid metabolites was observed, and Mogibacterium was correlated with most of bile acid metabolites (Figs. S3C–E).

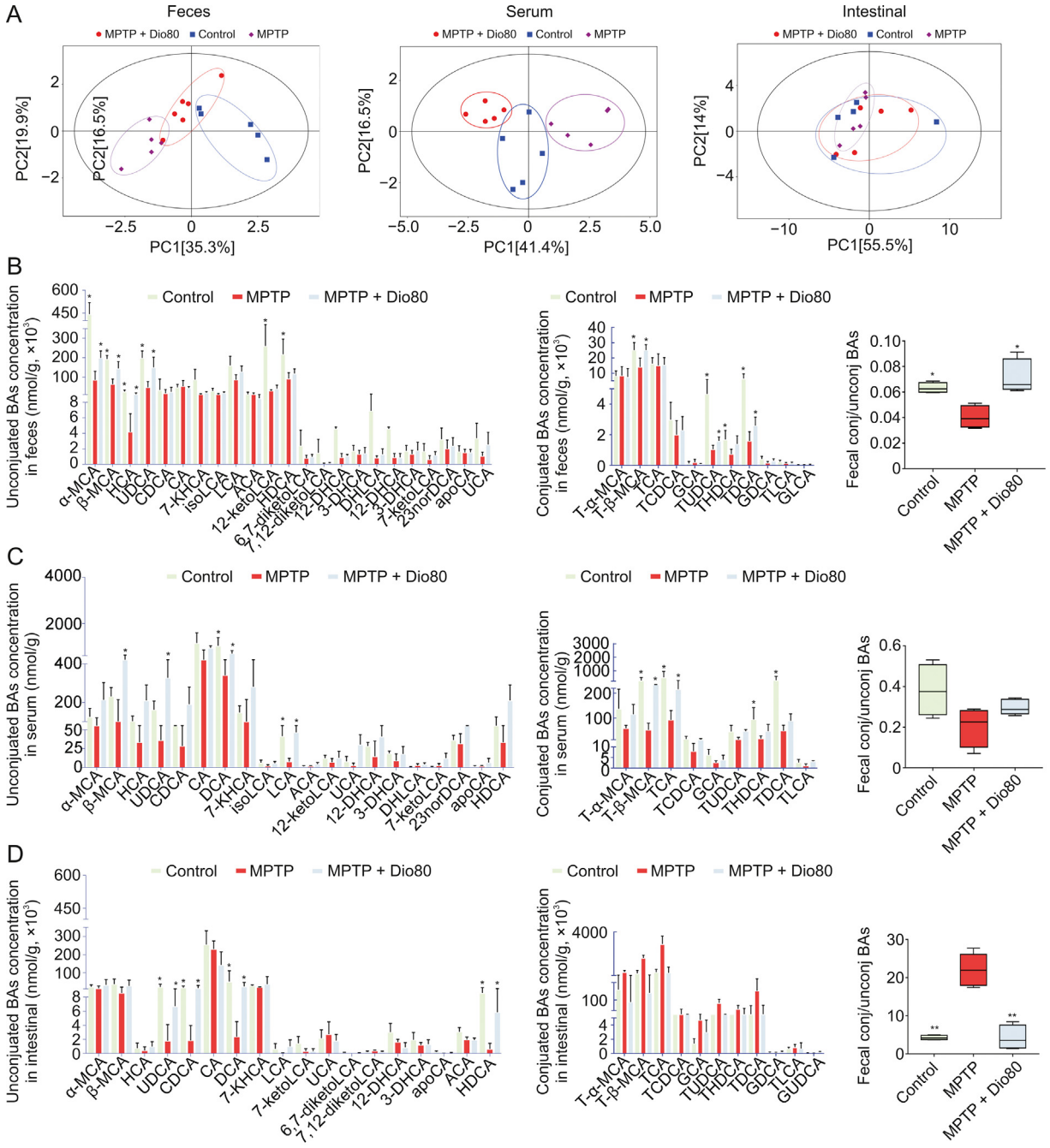

Fig. 6. Dioscin adjusts 1-methyl-4-phenyl-1,2,3,6-tetrahydropyridine (MPTP)-induced bile acid (BA) levels by targeted metabolomic analysis. (A) UniFrac distance-based principal coordinate analysis in feces, serum and intestine of control, MPTP and MPTP + Dio80. (B) Quantitative analysis of unconjuated BAs concentration and conjuaated BAs concentration in feces after disocin treatment on MPTP-induced Parkinson's disease (PD) mice. (C) Quantitative analysis of unconjugated BAs concentration and conjugated BAs concentration in serum after disocin treatment on MPTP-induced PD mice. (D) Quantitative analysis of unconjugated BAs concentration and conjugated BAs concentration in intestine after disocin treatment on MPTP-induced PD mice. All data are given as mean ± standard deviation (SD) ($n = 6$). $^{*}P < 0.05$ and $^{**}P < 0.01$ compared with MPTP group.

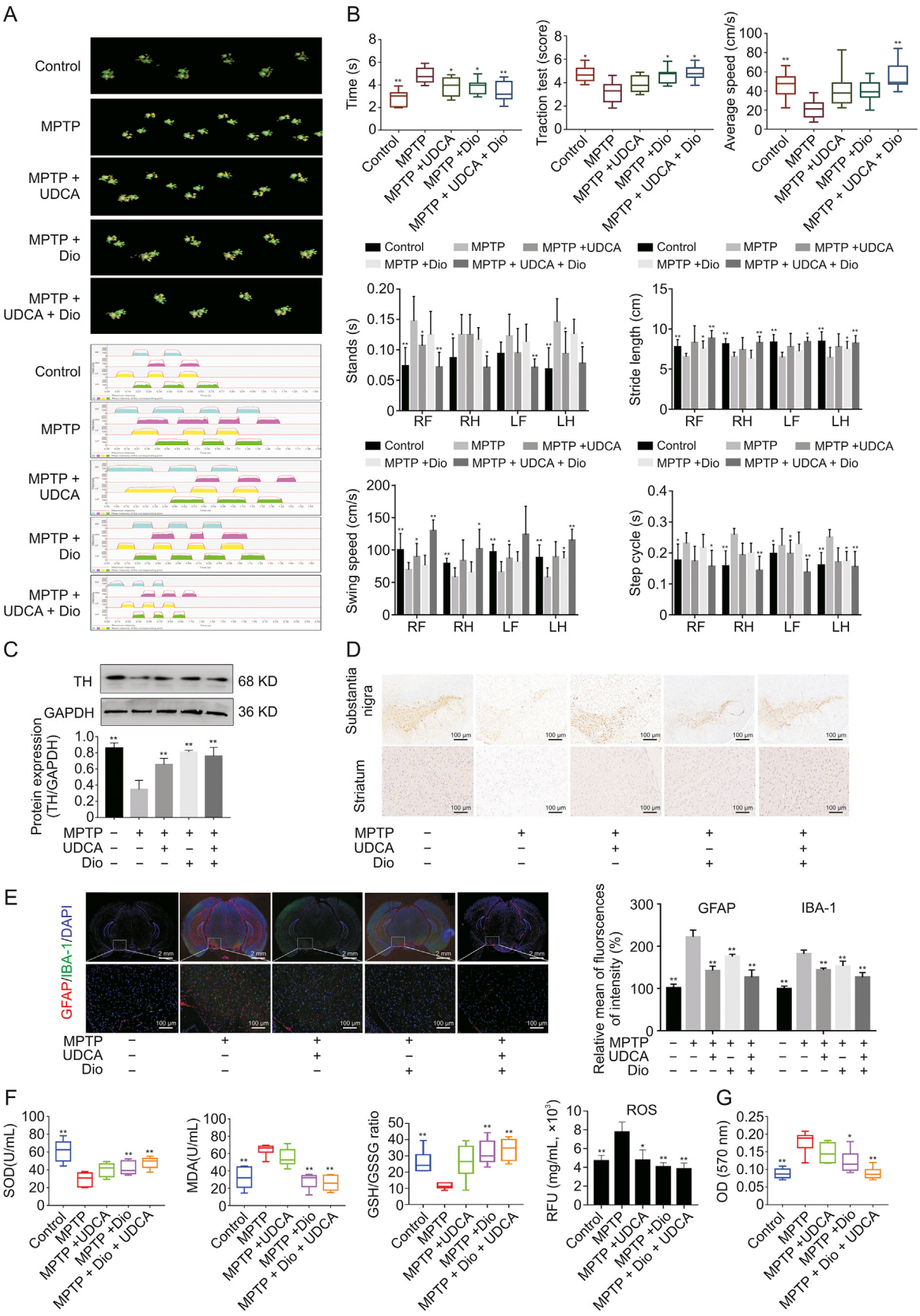

Fig. 7. Ursodeoxycholic acid (UDCA) enhances the protective effect of dioscin against Parkinson's disease (PD). (A) CatWalk print and mean intensity of the corresponding print of mice after dioscin and UDCA treatment on 1-methyl-4-phenyl-1,2,3,6-tetrahydropyridine (MPTP)-induced PD mice ($n = 8$). The upper panel (green prints in black background) shows the digitized prints, and the lower panel shows walking pattern and individual paws (RF: right front, RH: right hind, LF: left front, and LH: left hind). (B) Mice gait behavior

3.6. Dioscin altered MPTP-induced BA levels by targeted metabolomic analysis

Targeted metabolomics was applied to analyze the levels of BAs in feces, serum and intestine of mice. As shown in Fig. 6A, the results of UniFrac distance-based PCoA revealed that mice in the three groups had distinctly different patterns of BAs in feces and serum. However, no significant clustering of BA metabolites was found among the groups in intestine. Specifically, dioscin reversed the fecal concentrations of β-muricholic acid (β-MCA), hyocholic acid (HCA), ursodeoxycholic acid (UDCA), tauro-beta-muricholic acid (T-β-MCA), tauroursodeoxycholic acid (TUDCA) and taurodeoxycholic acid (TDCA) (Figs. 6B and S4A), the serum levels of β-MCA, HCA, UDCA, deoxycholic acid (DCA), lithocholic acid (LCA), T-β-MCA, TCA (Figs. 6C and S4B), and the intestinal levels of UDCA, TCA and TDCA (Figs. 6D and S4C). The fecal and serum cholic acid (CA)/DCA ratios in Fig. S4D showed that dioscin upregulated CA/DCA ratio. These results further indicated that reduced BSH activity by dioscin increased the levels of tauro-conjugated BAs. Interestingly, UDCA was the most variable bile acid in feces, serum and intestine (Fig. S4E).

3.7. UDCA mediated the therapeutic of dioscin in MPTP mice

As shown in Figs. 7A and B, traction test score, average speed, stride length, and swing speed were increased, whereas pole test time, stands and step cycle were decreased in MPTP + UDCA group and MPTP + UDCA + Dio group compared with MPTP group. In addition, the results in Figs. 7C and D revealed the increased level of TH in MPTP + UDCA group and MPTP + UDCA + Dio group compared with MPTP group. As shown in Figs. 7E–G, UDCA and dioscin administration decreased the levels of GFAP, IBA-1, MDA, ROS and BSH activity, while the levels of SOD and GSH/GSSG were increased in MPTP + Dio group and MPTP + UDCA + Dio group.

3.8. Dioscin promoted BAs-mediated GLP-1 pathway

As shown in Fig. 8A, the mRNA levels of *GLP-1* and the protein levels of GLP-1R in brain and intestine were upregulated by dioscin, and the protein level of TGR5 in intestine was also upregulated by dioscin. In addition, the brain protein or mRNA levels of NOX2, NF-κB, interleukin-6 (IL-6) and intercellular adhesion molecule (ICAM) were decreased, while the levels of SOD were increased by dioscin compared with MPTP group. In FMT test (Fig. 8B), the mRNA levels of *GLP-1* and the protein levels of GLP-1R in brain and intestine were increased in control-MPTP, Dio-MPTP, and MPTP + Dio-MPTP groups, and the protein level of TGR5 in intestine was also upregulated compared with MPTP-MPTP group. The levels of NOX2, NF-κB, IL-6 and ICAM were downregulated, while SOD was increased in control-MPTP, Dio-MPTP, and MPTP + Dio-MPTP groups compared with MPTP-MPTP group. Similar results were observed for UDCA treatment combined with dioscin in Fig. 8C. The combination of UDCA and dioscin slightly enhanced the therapeutic effect of dioscin. These results concluded that dioscin exerted *anti*-PD effects partially by adjusting BAs through GLP-1 signaling in a gut microbiota-dependent manner.

4. Discussion

Recently, development of drugs to treat PD has gained widely attention. Previous study has suggested that dioscin is an attractive candidate due to its potent protective effects against neurodegenerative disease. The classic animal model of PD is a neurotoxin model mainly targeting dopamine signaling, and conduction selective degeneration of substantia nigra dopamine neurons can be induced. MPTP is a highly lipophilic compound that can effectively penetrate BBB, and subsequently auto-oxidize to MPP^+. MPP^+ can decrease striatal dopamine levels within 12–72 h, and lead to the death of single nucleotide polymorphisms (SNPs) dopamine neurons. Thus, an acute PD model with a single high-dose injection and a chronic PD model with a long-term low-dose injection can all be established. Chronic or subacute models are generally preferred, because acute model has a higher mortality rate, and chronic model can be established after 2 weeks with the bradykinesia lasting for 6 months. Here, we used MPTP, an inhibitor of the mitochondrial complex that encompasses most of the pathological features of PD and enhances oxidative stress and neuroinflammation, to design an animal model [46]. The motor function tests showed that the mice in MPTP + Dio group exhibited shorter descent times in the pole test and higher scores in the traction test than those in MPTP group. In addition, there are numerous tests to assess crucial symptoms of PD, such as bradykinesia and gait disorders [47,48]. Previous studies have demonstrated that the CatWalk method can be used to analyze gait changes in 6-OHDA-induced rat models, and gait disorders and deficits in PD mouse models can also be sensitively evaluated [49,50]. In our study, the results showed that average speed, stride length and swing speeds, which are the major symptoms of PD, were significantly improved by dioscin. Moreover, the levels of stands, step cycles and base of support were decreased following dioscin treatment. These findings suggested that dioscin improved motor behavior. Furthermore, dioscin upregulated the expression of TH, an essential rate-limiting enzyme for the synthesis and release of DA and epinephrine, and activated astrocytes and microglia, suggesting that dioscin exerted its neuroprotective effects by inhibiting the activation of microglia and astrocytes.

Although some progress has been made in neurological diseases, the exact mechanism of PD and gut microbiota imbalance is still unclear. Previous studies have indicated that the genera Clostridium IV and Clostridium XVIII are enriched, while the genus Lactobacillus is reduced, and the relative abundance of Escherichia/Shigella are associated with disease duration [51,52]. However, a recent study has declared that the relative abundance of phylum *Firmicutes* and order *Clostridiales* were down-regulated, along with increased phylum *Proteobacteria* and *Enterobacteriales*, have been found in fecal samples of MPTP-induced PD mice [53]. In our study, we demonstrated that compared with MPTP group, dioscin upregulated the relative abundance of *Clostridiales* and *Enterobacteriales* on family level, and downregulated the relative levels of *Enterococcus*, *Streptococcus*, *Bacteroides* and *Lactobacillus* on genus level. Recently, a study has revealed that FMT can protect PD mice by suppressing neuroinflammation. Here, FMT fecal microbiota transplantation experiments showed that compared with

indicators change after dioscin and UDCA treatment on MPTP-induced PD mice, including pole test, traction test, average speed, stands, stride length, swing speeds, and step cycle ($n = 8$). (C) Western blotting assay of tyrosine hydroxylase (TH) in mice brain tissues after dioscin and UDCA treatment on MPTP-induced PD mice. (D) Immunohistochemistry assay of TH in mice brain tissues after dioscin and UDCA treatment on MPTP-induced PD mice. (E) Fluorescence semi-quantitative analysis of glial fibrillary acidic protein (GFAP) and ionized calcium bindingadaptor molecule-1 (IBA-1) expression after dioscin and UDCA treatment on MPTP-induced PD mice. (F) The levels of superoxide dismutase (SOD), malondialdehyde (MDA), glutathione (GSH)/glutathione synthase (GSS), reactive oxygen species (ROS) in mice brain tissues after dioscin and UDCA treatment on MPTP-induced PD mice. (G) The levels of fecal bile salt hydrolase (BSH) activity after dioscin and UDCA treatment on MPTP-induced PD mice. All data are presented as mean ± standard deviation (SD) ($n \geq 3$). $^{*}P < 0.05$ and $^{**}P < 0.01$ compared with MPTP group.

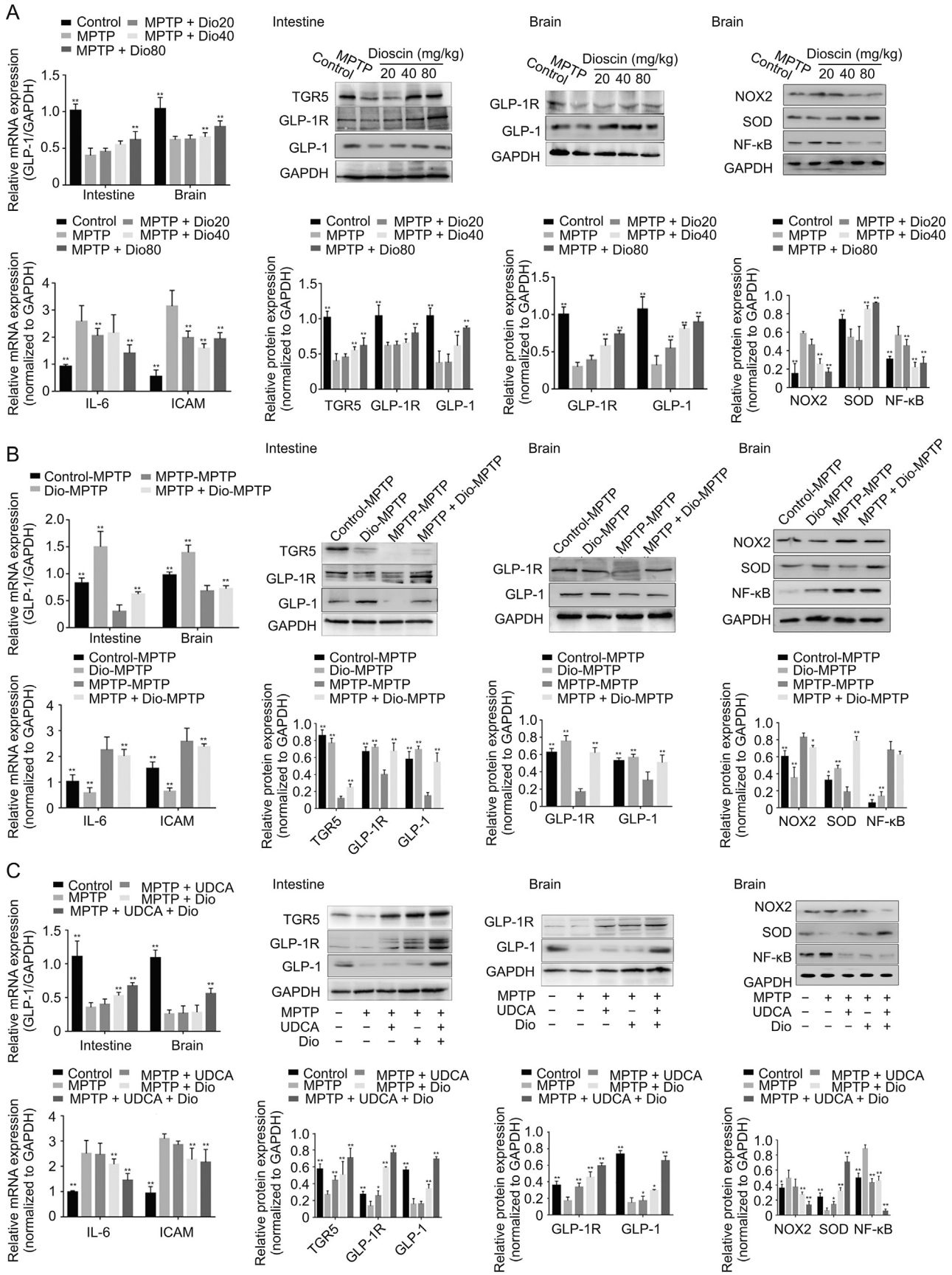

Fig. 8. Dioscin suppresses bile acids (BAs)-mediated oxidative stress and neuroinflammation via adjusting glucagon-like peptide-1 (GLP-1) signal. (A) The mRNA levels of GLP-1 in intestine and brain, protein expression levels of takeda G protein-coupled receptor 5 (TGR5), glucagon-like peptide-1 receptor (GLP-1R), GLP-1 in intestine, mRNA levels of interleukin-6 (IL-6), intercellular adhesion molecule (ICAM) in brain, and protein expression levels of GLP-1R, GLP-1, down-regulated NADPH oxidases 2 (NOX2), superoxide dismutase (SOD),

MPTP-MPTP, MPTP + dioscin administration restored gait disorder and behavioral abnormalities in mice, which also inhibited microglial activation and upregulated TH expression. Moreover, FMT from control mice and Dio-dosed mice also recovered the evaluation index, which was consistent with previous results [54]. Interestingly, FMT from Dio-dosed mice even improved gait disorder more profoundly than FMT from any other group, which demonstrated that dioscin exerted its *anti*-PD effects by remodeling gut microbiota. Simultaneously, this may be the reason that dioscin had low bioavailability in humans but played a noticeable role in indigenous biological activities.

In recent years, studies on the relationship between gut microbiota and host have confirmed that intestinal flora and metabolites are closely related to human diseases and health [55]. LC-MS is highly sensitive that can separate thousands of small molecule metabolites with low detection limits. GC-MS is an important method for the analysis of volatile or semi-volatile small molecular compounds. Hence, GC-MS can be used as a supplement to test heat stable compounds for non-targeted metabolomics. In addition, the databases used by GC-MS and LC-MS are not the same, and thus we used the two methods simultaneously to find more differential metabolites. In our study, a total of over 600 differential metabolites were detected in feces, and we observed that some metabolic pathways, including steroid and primary bile acid biosynthesis, were closely related to therapeutic interventions of dioscin. Moreover, the levels of cholic acid and deoxycholic acid were obviously upregulated, and the levels of taurodeoxycholic acid, taurolithocholic acid and tauroursodeoxycholic acid were significantly decreased in the feces of MPTP group compared to control mice, while dioscin alleviated the situation. Additionally, most of the differential bacteria can encode BSH, which can maintain the balance of BA metabolism by catalyzing the hydrolysis of conjugated bile salts into deconjugated BAs [56]. Previous studies have revealed that the regulation of microbes associated with BSH can attenuate hypercholesterolemia in high-fat diet mice and characterize aging-related disorders in a mouse model [57,58]. Our data suggested that dioscin directly inhibited the activity of BSH enzyme in feces, indicating that the compound improved the relative abundance of these BSH-coding bacteria to alter the levels of BAs. In a subsequent study, targeted metabolomics revealed a remarkable changes of BAs levels in dioscin-treated feces and serum. Remarkably, 41 BAs were quantified, and 4 BAs including UDCA, TUDCA, TDCA and β-MCA were changed. A previous study has shown that UDCA can increase the striatal dopamine content and improve mitochondrial function in a rotenone PD rat model [18]. Our results showed that ursodeoxycholic acid markedly alleviated motor deficits and microglial activation, upregulated TH expression, inhibited oxidative stress and neuroinflammation, and improved the protective effects of dioscin against PD in mice. Interestingly, dioscin significantly increased the conjugated BA/unconjugated BA ratio in feces which was consistent with the results of BSH activity. In addition, we found that the fecal and serum CA/DCA ratios were slightly increased after dioscin administration, indicating that dioscin affected 7-α-dehydroxylation activity. It is known that endogenous UDCA is a secondary bile acid formed by 7-hydroxysteroid dehydrogenase (7-HSDH) regulated by gut microbiome, which can isomerize 7α-hydroxy of urodeoxycholic acid into 7β-hydroxy. In addition, glycoursodeoxycholic acid (GUDCA) and TUDCA secreted by bile also hydrolyze into UDCA under the action of BSH [59]. In our work, the significant changes of UDCA may be due to the effect of dioscin on the common activity of BSH and 7-α-dehydroxylationc, and this conclusion is needed further demonstration. In addition, previous research has suggested that glycoside-type compound of dioscin can present in low amounts in plasma and urine of rats [60], and most of it is excreted from the intestine in a prototype mode. Importantly, dioscin nearly cannot pass BBB to brain. Furthermore, some reports have revealed that more kinds of metabolites can be found in feces than in plasma, while the fewest kinds of metabolites can be detected in urine [61,62], which was consistent with our sequencing results.

At present, there are two bile acid indirect pathways in the central system, including FXR-FGF19 pathway and TGR5-GLP-1 pathway. In intestine, a specific group of L-cells, enteroendocrine cells, can produce GLP-1 upon the activation of TGR5, which can be triggered by bile acids. As the well-studied bile acid receptor, stimulation of TGR5 by bile acids can also cause the release of gut hormone GLP-1, which is capable of extending the bile acid signal from the intestine to other parts of body [63]. Interestingly, a recent study has demonstrated that binding TUDCA to TGR5 has anti-inflammatory effect on acute brain inflammation, suggesting the neuroprotective effect of TUDCA for neurodegenerative diseases. In the present work, the levels of TGR5 were activated by dioscin to stimulate the secretion of GLP-1 in intestinal. GLP-1 is a pleiotropic hormone with broad pharmacological potential, including obesity, diabetes, and neurodegenerative disorders, and GLP-1 analogs have been used for the treatment of PD [64,65]. It has been reported that the probiotics *Clostridium butyricum* can ameliorate motor deficits in a mouse model via gut microbiota-GLP-1 pathway, suggesting that GLP-1 is related to PD pathogenesis [66]. Of note, GLP-1 receptor analogs can improve SH-SY5Y cell viability, normalize ROS and attenuate reactive astrocytes, further illustrating that GLP-1 pathway can be regarded as an effective treatment on oxidative damage and neuroinflammation [67]. GLP-1 receptor agonist can affect the pathogenesis of neurodegenerative diseases [68]. In addition, GLP-1 receptor agonists can regulate dopamine levels in PD [69], which can further demonstrate the neuroprotective effects of GLP-1 in PD. In our study, we provided the evidences that the levels of GLP-1 and GLP-1R in the brain and intestine were upregulated by dioscin, and the compound elevated the levels of SOD and decreased the protein or mRNA levels of NOX2, NF-κB, IL-6 and ICAM, leading to an evident inhibition of neuroinflammation and oxidative stress. Furthermore, similar results were shown in FMT test and UDCA combined with dioscin treatment. These findings elucidated that the *anti*-PD effect of dioscin was achieved by adjusting BAs through GLP-1 signaling in a gut microbiota-dependent manner. Several studies have proven the protective effects of dioscin against some diseases, and various approaches have confirmed the advantages of natural products over commercially available drugs, indicating that dioscin has the potential to be further incorporated into clinical practice [70]. Di-Ao-Xin-Xue-Kang capsule containing dioscin has been applied to cure cardiovascular disease for more than 20 years in China. The rhizomes of *D. zingiberensis C. H.* Wright has been used as one famous traditional medicine [71], whereas dioscin-containing DA-9801 has

nuclear factor-kappaB (NF-κB) in brain after dioscin treatment on MPTP-induced Parkinson's disease (PD) model. Data are presented as mean ± standard deviation (SD) ($n = 3$). $^{*}P < 0.05$ and $^{**}P < 0.01$ compared with MPTP group. (B) The mRNA levels of GLP-1 in intestine and brain, protein expression levels of TGR5, GLP-1R, GLP-1 in intestine, mRNA levels of IL-6, ICAM in brain, and protein expression levels of GLP-1R, GLP-1, NOX2, SOD, NF-κB in brain after fecal transplantation from dioscin-treated mice to MPTP mice. Data are presented as mean ± SD ($n = 3$). $^{*}P < 0.05$ and $^{**}P < 0.01$ compared with MPTP-MPTP group. (C) The mRNA levels of GLP-1 in intestine and brain, protein expression levels of TGR5, GLP-1R, GLP-1 in intestine, mRNA levels of IL-6, ICAM in brain, and protein expression levels of GLP-1R, GLP-1, NOX2, SOD, NF-κB in brain after dioscin and ursodeoxycholic acid (UDCA) treatment on MPTP-induced PD model. Data are presented as mean ± SD ($n = 3$). $^{*}P < 0.05$ and $^{**}P < 0.01$ compared with MPTP group.

completed phase II clinical trials for treating diabetic neuropathy [72]. However, the most currently available pharmacodynamic and mechanistic data are derived from in vitro and in vivo experiments, which are required additional works before dioscin can be used to treat human diseases.

5. Conclusions

This study showed that dioscin remodeled gut microbiota and regulated bile acid-mediated oxidative stress and neuroinflammation by targeting GLP-1 signaling. The data also indicated that gut microbiota and bile acid may become interesting targets for PD therapy. Dioscin should be considered a potent candidate, and however, further studies are warranted to investigate the specific strains and the exact roles of bile acids during PD with or without dioscin treatments.

CRediT author statement

Zhang Mao: Methodology, Investigation, Validation, Writing - Original draft preparation; **Haochen Hui**: Investigation, Validation, Data curation, Formal analysis; **Xuerong Zhao**: Conceptualization, Methodology, Visualization; **Lina Xu**: Visualization, Formal analysis, Data curation; **Yan Qi**: Formal analysis, Data curation, Software, Validation; **Lianhong Yin**: Resources, investigation, Writing - Reviewing and Editing; **Liping Qu**: Resources, Supervision, Visualization; **Lan Han**: Conceptualization, Resources, Supervision, Visualization; **Jinyong Peng**: Conceptualization, Resources, Project administration, Writing - Reviewing and Editing.

Declaration of competing interest

The authors declare that there are no conflicts of interest.

Acknowledgments

The authors gratefully acknowledge funding from the Spring City Plan: The High-Level Talent Promotion and Training Project of Kunming and the Independent Research Fund of Yunnan Characteristic Plant Extraction Laboratory (Grant No.: 2022YKZY001).

Appendix A. Supplementary data

Supplementary data to this article can be found online at https://doi.org/10.1016/j.jpha.2023.06.007.

References

[1] Y. Chandrasekhar, G. Phani Kumar, E.M. Ramya, et al., Gallic acid protects 6-OHDA induced neurotoxicity by attenuating oxidative stress in human dopaminergic cell line, Neurochem. Res. 43 (2018) 1150–1160.
[2] P. Gan, L. Ding, G. Hang, et al., Oxymatrine attenuates dopaminergic neuronal damage and microglia-mediated neuroinflammation through cathepsin D-dependent HMGB1/TLR4/NF-κB pathway in Parkinson's disease, Front. Pharmacol. 11 (2020) 776–776.
[3] S. Peng, B. Zhang, J. Yao, et al., Dual protection of hydroxytyrosol, an olive oil polyphenol, against oxidative damage in PC12 cells, Food Funct. 6 (2015) 2091–2100.
[4] J.L. Ilkiw, L.C. Kmita, A.D.S. Targa, et al., Dopaminergic lesion in the olfactory bulb restores olfaction and induces depressive-like behaviors in a 6-OHDA model of Parkinson's disease, Mol. Neurobiol. 56 (2019) 1082–1095.
[5] J. Lee, K. Song, E. Huh, et al., Neuroprotection against 6-OHDA toxicity in PC12 cells and mice through the Nrf2 pathway by a sesquiterpenoid from Tussilago farfara, Redox Biol. 18 (2018) 6–15.
[6] H. Li, Z. Tang, P. Chu, et al., Neuroprotective effect of phosphocreatine on oxidative stress and mitochondrial dysfunction induced apoptosis *in vitro* and *in vivo*: Involvement of dual PI3K/Akt and Nrf2/HO-1 pathways, Free Radic. Biol. Med. 120 (2018) 228–238.
[7] C. Zhang, C. Li, S. Chen, et al., Berberine protects against 6-OHDA-induced neurotoxicity in PC12 cells and zebrafish through hormetic mechanisms involving PI3K/AKT/Bcl-2 and Nrf2/HO-1 pathways, Redox Biol. 11 (2017) 1–11.
[8] C. van der Merwe, H.C. van Dyk, L. Engelbrecht, et al., Curcumin rescues a PINK1 knock down SH-SY5Y cellular model of Parkinson's disease from mitochondrial dysfunction and cell death, Mol. Neurobiol. 54 (2017) 2752–2762.
[9] M.R. de Oliveira, A. Peres, G.C. Ferreira, et al., Carnosic acid protects mitochondria of human neuroblastoma SH-SY5Y cells exposed to paraquat through activation of the Nrf2/HO-1 axis, Mol. Neurobiol. 54 (2017) 5961–5972.
[10] A. Romero, E. Ramos, I. Ares, et al., Oxidative stress and gene expression profiling of cell death pathways in alpha-cypermethrin-treated SH-SY5Y cells, Arch. Toxicol. 91 (2017) 2151–2164.
[11] C. Qiao, Q. Zhang, Q. Jiang, et al., Inhibition of the hepatic Nlrp3 protects dopaminergic neurons via attenuating systemic inflammation in a MPTP/p mouse model of Parkinson's disease, J. Neuroinflammation 15 (2018) 193–193.
[12] J.R. Bedarf, F. Hildebrand, L.P. Coelho, et al., Functional implications of microbial and viral gut metagenome changes in early stage L-DOPA-naïve Parkinson's disease patients, Genome Med. 9 (2017), 39.
[13] E.M. Hill-Burns, J.W. Debelius, J.T. Morton, et al., Parkinson's disease and Parkinson's disease medications have distinct signatures of the gut microbiome, Mov. Disord. 32 (2017) 739–749.
[14] M.M. Unger, J. Spiegel, K.U. Dillmann, et al., Short chain fatty acids and gut microbiota differ between patients with Parkinson's disease and age-matched controls, Parkinsonism Relat. Disord. 32 (2016) 66–72.
[15] X. Qi, C. Yun, L. Sun, et al., Gut microbiota-bile acid-interleukin-22 axis orchestrates polycystic ovary syndrome, Nat. Med. 25 (2019) 1225–1233.
[16] Z. Song, Y. Cai, X. Lao, et al., Taxonomic profiling and populational patterns of bacterial bile salt hydrolase (BSH) genes based on worldwide human gut microbiome, Microbiome 7 (2019), 9.
[17] A. Luxenburger, H. Clemmens, C. Hastings, et al., 3α,7-Dihydroxy-14(13→12) abeo-5β, 12α(H),13β(H)-cholan-24-oic acids display neuroprotective properties in common forms of Parkinson's disease, Biomolecules 13 (2022), 76.
[18] W.J. Griffiths, J. Abdel-Khalik, E. Yutuc, et al., Concentrations of bile acid precursors in cerebrospinal fluid of Alzheimer's disease patients, Free Radic. Biol. Med. 134 (2019) 42–52.
[19] A. Heinken, D.A. Ravcheev, F. Baldini, et al., Systematic assessment of secondary bile acid metabolism in gut microbes reveals distinct metabolic capabilities in inflammatory bowel disease, Microbiome 7 (2019), 75.
[20] N.F. Abdelkader, M.M. Safar, H.A. Salem, Ursodeoxycholic acid ameliorates apoptotic cascade in the rotenone model of Parkinson's disease: Modulation of mitochondrial perturbations, Mol. Neurobiol. 53 (2016) 810–817.
[21] M. Castro-Caldas, A.N. Carvalho, E. Rodrigues, et al., Tauroursodeoxycholic acid prevents MPTP-induced dopaminergic cell death in a mouse model of Parkinson's disease, Mol. Neurobiol. 46 (2012) 475–486.
[22] F. Reimann, A.M. Habib, G. Tolhurst, et al., Glucose sensing in L cells: A primary cell study, Cell Metab. 8 (2008) 532–539.
[23] S. Fukuda, S. Nakagawa, R. Tatsumi, et al., Glucagon-like peptide-1 strengthens the barrier integrity in primary cultures of rat brain endothelial cells under basal and hyperglycemia conditions, J. Mol. Neurosci. 59 (2016) 211–219.
[24] W. Liu, J. Jalewa, M. Sharma, et al., Neuroprotective effects of lixisenatide and liraglutide in the 1-methyl-4-phenyl-1,2,3,6-tetrahydropyri-dine mouse model of Parkinson's disease, Neuroscience 303 (2015) 42–50.
[25] G. Yoon, Y.K. Kim, J. Song, Glucagon-like peptide-1 suppresses neuroinflammation and improves neural structure, Pharmacol. Res. 152 (2019), 104615.
[26] S.L. Wu, C.C. Zhang, J.J. Chen, et al., Oligostilbenes from the seeds of Paeonia lactiflora as potent GLP-1 secretagogues targeting TGR5 receptor, Fitoterapia 163 (2022), 105336.
[27] R.G. Abdel-Latif, G.H. Heeba, A. Taye, et al., Lixisenatide, a novel GLP-1 analog, protects against cerebral ischemia/reperfusion injury in diabetic rats, Naunyn Schmiedebergs Arch. Pharmacol. 391 (2018) 705–717.
[28] M. Mohammed El Tabaa, A. Anis, R. Mohamed Elgharabawy, et al., GLP-1 mediates the neuroprotective action of crocin against cigarette smoking-induced cognitive disorders via suppressing HMGB1-RAGE/TLR4-NF-kappaB pathway, Int. Immunopharmacol. 110 (2022), 108995.
[29] H. Chen, L. Xu, L. Yin, et al., iTRAQ-based proteomic analysis of dioscin on human HCT-116 colon cancer cells, Proteomics 14 (2014) 51–73.
[30] L. Lv, L. Zheng, D. Dong, et al., Dioscin, a natural steroid saponin, induces apoptosis and DNA damage through reactive oxygen species: A potential new drug for treatment of glioblastoma multiforme, Food Chem. Toxicol. 59 (2013) 657–669.
[31] X. Tao, X. Wan, Y. Xu, et al., Dioscin attenuates hepatic ischemia-reperfusion injury in rats through inhibition of oxidative-nitrative stress, inflammation and apoptosis, Transplantation 98 (2014) 604–611.
[32] X. Tao, X. Sun, L. Yin, et al., Dioscin ameliorates cerebral ischemia/reperfusion injury through the downregulation of TLR4 signaling via HMGB-1 inhibition, Free Radic. Biol. Med. 84 (2015) 103–115.
[33] Y. Qi, R. Li, L. Xu, et al., Neuroprotective effect of dioscin on the aging brain, Molecules 24 (2019), 1247.
[34] A.C.V. de Guzman, M.A. Razzak, B. Purevdulam, et al., Anti-Parkinson's disease function of Dioscin-Zein-Carboxymethyl cellulose nanocomplex in caenorhabditis elegans, Biotechnol. J. 15 (2020), 2000080.
[35] K. Li, Y. Tang, J.P. Fawcett, et al., Characterization of the pharmacokinetics of dioscin in rat, Steroids 70 (2005) 525–530.

[36] S. Jin, T. Guan, S. Wang, et al., Dioscin alleviates cisplatin-induced mucositis in rats by modulating gut microbiota, enhancing intestinal barrier function and attenuating TLR4/NF-κB signaling cascade, Int. J. Mol. Sci. 23 (2022), 4431.
[37] B. Ren, S. Fu, Y. Liu, et al., Dioscin ameliorates slow transit constipation in mice by up-regulation of the BMP2 secreted by muscularis macrophages, Iran. J. Basic Med. Sci. 25 (2022) 1132–1140.
[38] Y. Liu, K. Chen, F. Li, et al., Probiotic lactobacillus rhamnosus GG prevents liver fibrosis through inhibiting hepatic bile acid synthesis and enhancing bile acid excretion in mice, Hepatology 71 (2020) 2050–2066.
[39] J. Sun, J. Xu, Y. Ling, et al., Fecal microbiota transplantation alleviated Alzheimer's disease-like pathogenesis in APP/PS1 transgenic mice, Transl. Psychiat. 9 (2019) 189–189.
[40] W.B. Dunn, D. Broadhurst, P. Begley, et al., Procedures for large-scale metabolic profiling of serum and plasma using gas chromatography and liquid chromatography coupled to mass spectrometry, Nat. Protoc. 6 (2011) 1060–1083.
[41] T. Kind, G. Wohlgemuth, D.Y. Lee, et al., FiehnLib: Mass spectral and retention index libraries for metabolomics based on quadrupole and time-of-flight gas chromatography/mass spectrometry, Anal. Chem. 81 (2009) 10038–10048.
[42] C.A. Smith, E.J. Want, G. O'Maille, et al., XCMS: Processing mass spectrometry data for metabolite profiling using nonlinear peak alignment, matching, and identification, Anal. Chem. 78 (2006) 779–787.
[43] S. Kapoor, M. Fitzpatrick, E. Clay, et al., Metabolomics in the Analysis of Inflammatory Diseases, in: U. Roessner (Ed.), Metabolomics, InTech, Rijeka (HR), 2012.
[44] R.M. Uppu, D. Woods, N.L. Parinandi, Measurement of Oxidative Stress Status in Human Populations: A Critical Need for a Metabolomic Profiling, in: L.J. Berliner, N.L. Parinandi (Eds.), Measuring Oxidants and Oxidative Stress in Biological Systems, Springer Nature Switzerland AG., Cham (CH), 2020, pp. 123–131.
[45] J. Wang, T. Zhang, X. Shen, et al., Serum metabolomics for early diagnosis of esophageal squamous cell carcinoma by UHPLC-QTOF/MS, Metabolomics 12 (2016), 116.
[46] K.E.W. Vendrik, R.E. Ooijevaar, P.R.C. de Jong, et al., Fecal microbiota transplantation in neurological disorders, Front. Cell. Infect. Microbiol. 10 (2020), 98.
[47] C.S. Chuang, J.C. Chang, F.C. Cheng, et al., Modulation of mitochondrial dynamics by treadmill training to improve gait and mitochondrial deficiency in a rat model of Parkinson's disease, Life Sci. 191 (2017) 236–244.
[48] M. Shah, S. Rajagopalan, L. Xu, et al., The high-affinity D2/D3 agonist D512 protects PC12 cells from 6-OHDA-induced apoptotic cell death and rescues dopaminergic neurons in the MPTP mouse model of Parkinson's disease, J. Neurochem. 131 (2014) 74–85.
[49] C.S. Chuang, H.L. Su, F.C. Cheng, et al., Quantitative evaluation of motor function before and after engraftment of dopaminergic neurons in a rat model of Parkinson's disease, J. Biomed. Sci. 17 (2010), 9.
[50] A.R. Tsang, N. Rajakumar, M.S. Jog, Intrapallidal injection of botulinum toxin A recovers gait deficits in a parkinsonian rodent model, Acta Physiol. 226 (2019), e13230.
[51] Y. Qian, X. Yang, S. Xu, et al., Alteration of the fecal microbiota in Chinese patients with Parkinson's disease, Brain Behav. Immun. 70 (2018) 194–202.
[52] H. Xiao, M. Li, J. Cai, et al., Selective cholinergic depletion of pedunculopontine tegmental nucleus aggravates freezing of gait in parkinsonian rats, Neurosci. Lett. 659 (2017) 92–98.
[53] X. Yang, Y. Qian, S. Xu, et al., Longitudinal analysis of fecal microbiome and pathologic processes in a rotenone induced mice model of Parkinson's disease, Front. Aging Neurosci. 9 (2017), 441.
[54] M.F. Sun, Y.L. Zhu, Z.L. Zhou, et al., Neuroprotective effects of fecal microbiota transplantation on MPTP-induced Parkinson's disease mice: Gut microbiota, glial reaction and TLR4/TNF-α signaling pathway, Brain Behav. Immun. 70 (2018) 48–60.
[55] Z.L. Zhou, X.B. Jia, M.F. Sun, et al., Neuroprotection of fasting mimicking diet on MPTP-Induced Parkinson's disease mice via gut microbiota and metabolites, Neurotherapeutics 16 (2019) 741–760.
[56] K.L. Mertens, A. Kalsbeek, M.R. Soeters, et al., Bile acid signaling pathways from the enterohepatic circulation to the central nervous system, Front. Neurosci. 11 (2017) 617–617.
[57] J. Hertel, A.C. Harms, A. Heinken, et al., Integrated analyses of microbiome and longitudinal metabolome data reveal microbial-host interactions on sulfur metabolism in Parkinson's disease, Cell Rep. 29 (2019) 1767–1777.
[58] F. Huang, X. Zheng, X. Ma, et al., Theabrownin from Pu-erh tea attenuates hypercholesterolemia via modulation of gut microbiota and bile acid metabolism, Nat. Commun. 10 (2019), 4971.
[59] Z. Araya, K. Wikvall, 6α-Hydroxylation of taurochenodeoxycholic acid and lithocholic acid by CYP3A4 in human liver microsomes, BBA-Mol. Cell Biol. Lipids 1438 (1999) 47–54.
[60] Y.N. Tang, Y.X. Pang, X.C. He, et al., UPLC-QTOF-MS identification of metabolites in rat biosamples after oral administration of Dioscorea saponins: A comparative study, J. Ethnopharmacol. 165 (2015) 127–140.
[61] V.K. Manda, B. Avula, Z. Ali, et al., Characterization of in vitro ADME properties of diosgenin and dioscin from Dioscorea villosa, Planta Med. 79 (2013) 1421–1428.
[62] H. Zhu, J.-D. Xu, Q. Mao, et al., Metabolic profiles of dioscin in rats revealed by ultra-performance liquid chromatography quadrupole time-of-flight mass spectrometry, Biomed. Chromatogr. 29 (2015) 1415–1421.
[63] N. Yanguas-Casás, M.A. Barreda-Manso, M. Nieto-Sampedro, et al., TUDCA: An agonist of the bile acid receptor GPBAR1/TGR5 with anti-inflammatory effects in microglial cells, J. Cell Physiol. 232 (2017) 2231–2245.
[64] T.D. Müller, B. Finan, S.R. Bloom, et al., Glucagon-like peptide 1 (GLP-1), Mol. Metab. 30 (2019) 72–130.
[65] X. Zheng, T. Chen, R. Jiang, et al., Hyocholic acid species improve glucose homeostasis through a distinct TGR5 and FXR signaling mechanism, Cell Metab. 33 (2021) 791–803.
[66] J. Sun, H. Li, Y. Jin, et al., Probiotic Clostridium butyricum ameliorated motor deficits in a mouse model of Parkinson's disease via gut microbiota-GLP-1 pathway, Brain Behav. Immun. 91 (2021) 703–715.
[67] G.N. Salles, M.L. Calió, C. Hölscher, et al., Neuroprotective and restorative properties of the GLP-1/GIP dual agonist DA-JC1 compared with a GLP-1 single agonist in Alzheimer's disease, Neuropharmacology 162 (2020), 107813.
[68] J.K. Sterling, M.O. Adetunji, S. Guttha, et al., GLP-1 receptor agonist NLY01 reduces retinal inflammation and neuron death secondary to ocular hypertension, Cell Rep. 33 (2020), 108271.
[69] M.K. Mahapatra, M. Karuppasamy, B.M. Sahoo, Therapeutic potential of semaglutide, a newer GLP-1 receptor agonist, in abating obesity, non-alcoholic steatohepatitis and neurodegenerative diseases: A narrative review, Pharm. Res. 39 (2022) 1233–1248.
[70] S. Bandopadhyay, U. Anand, V.S. Gadekar, et al., Dioscin: A review on pharmacological properties and therapeutic values, Biofactors 48 (2022) 22–55.
[71] X. Zhang, M. Jin, N. Tadesse, et al., Dioscorea zingiberensis C. H. Wright: An overview on its traditional use, phytochemistry, pharmacology, clinical applications, quality control, and toxicity, J. Ethnopharmacol. 220 (2018) 283–293.
[72] L. Yang, S. Ren, F. Xu, et al., Recent advances in the pharmacological activities of Dioscin, Biomed Res. Int. 2019 (2019), 5763602.